Local approach for prediction of ductile fracture initiation in welded specimens

B. Younise [1,*], M. Rakin [2], B. Medjo [2], A. Sedmak [1]

[1]Faculty of Mechanical Engineering, University of Belgrade, Serbia
[2]Faculty of Technology and Metallurgy, University of Belgrade, Serbia

Keywords

Ductile fracture, local approach, welded joint.

1. Introduction

Due to the nature of the welding process, the welded zone contains, in general, more flaws and defects than the surrounding base material and it is a critical place for fracture. The weld metal, heat affected zone and the base material will have different material properties, and this mismatch in strength will influence the failure conditions.

Ductile fracture of metallic involves micro-void nucleation and growth, and final coalescence of neighbouring voids to create new surfaces of a macro-crack.

Local approach has been extensively used in the last decade in order to analyse and predict ductile fracture initiation of alloys. A large number of models have been developed to analysis ductile fracture, these models link material fracture behaviour to the parameters that describe the evolution of micro-voids rather than the conventional global fracture parameters which can not be directly transferred from one geometry to the another. Ductile failure process for porous materials often modelled by means of the Gurson model [1], which is one of the most widely known micro-mechanical models for ductile fracture, and describes the progressive degradation of material stress capacity. In this model, which is a modification of the von Mises one, an elastic-plastic matrix material is considered and a new internal variable, the void volume fraction, f, is introduced. The original Gurson model was later modified by many authors, particularly by Tvergaard and Needleman, and is known GTN model [2].

In this paper, the effect of strength mismatch and width of welded joints on the ductile fracture behaviour has been investigated by using two types of welded specimens; single-edge notched bend, SE(B), and compact tension, C(T), specimens. The transferability of ductile fracture initiation parameter between two specimens has been discussed. The two types of welded specimens made of high-strength low alloyed (HSLA) steel have been used to analyse the effect of constraint in case of over-matched, OM, and under-matched, UM, welded joints. Micro-mechanical GTN model was applied in order to predict the crack growth initiation and to analyse the transferability of ductile fracture parameters between welded specimens.

*) Corresponding author
E-mail address: bashiryounise@yahoo.com

2. Modelling of ductile fracture

Ductile damage develops through three stages: nucleation, growth and coalescence of voids, resulting in final failure [3]. Growth of nucleated voids is strongly dependent on stress and strain state. Most experiments and analysis show an exponential increase with the stress triaxiality, which defined as the ratio of the mean stress, σ_m to the equivalent stress, σ_{eq}. Ductile fracture models may be classified in two groups: uncoupled micro-mechanical models and coupled micro-mechanical models. In uncoupling modelling, void presence does not significantly alter the behaviour of material [4], so the model does not include the damage parameter and von Mises criterion is most frequently used as a yield criterion, while the coupled micro-mechanical model considers material as a porous medium where the influence of nucleated voids on the stress-strain state and plastic flow can not be avoided. The GTN (Gurson-Tvergard -Needleman) model is based on the hypothesis that the void nucleation and growth in a metal may be macroscopically described by extending the von Mises plasticity theory to cover the effects of porosity occurring in the material. The void volume fraction , f, as a variable is introduced into the expression for the plastic potential [1]:

$$\phi = \frac{3S_{ij}S_{ij}}{2\sigma_{eq}^2} + 2q_1 f^* \cosh\left(\frac{3q_2\sigma_m}{2\sigma_{eq}}\right) - \left[1 + \left(q_1 f^*\right)^2\right] = 0 \quad (1)$$

where σ_{eq} denotes the yield stress of the material matrix, σ_m is mean stress, S_{ij} is the stress deviator, the parameters q_1 and q_2 were introduced by Tvergaard [5] to improve the ductile fracture prediction of the Gurson model and f^* is the damage function [2]:

$$f^* = \begin{cases} f & for \quad f \le f_c \\ f_c + K(f - f_c) & for \quad f > f_c \end{cases} \quad (2)$$

where f_c is the critical void volume fraction at moment of void coalescence occurs. For $f^* = 0$, the plastic potential (Eq. (1)) is identical with that of von Mises. The parameter K defines the slope of sudden drop of the force on the force-diameter reduction diagram, and is often referred to as "accelerating factor".

In ductile steel, the voids nucleate due to separation or fracture of non-metallic inclusions and secondary-phase particles from the material matrix. Two phenomena contribute to the increase of the void volume fraction in FE analysis with the embedded GTN yield criterion: one is the growth of the existing voids and the other is the nucleation of new voids under external loading:

$$\dot{f} = \dot{f}_{nucleation} + \dot{f}_{growth} \tag{3}$$

$$\dot{f}_{nucleation} = A\dot{\varepsilon}^{p}_{eq} \tag{4}$$

$$\dot{f}_{growth} = (1-f)\dot{\varepsilon}^{p}_{ii} \tag{5}$$

where $\dot{\varepsilon}^{p}_{eq}$ is the equivalent plastic strain rate, $\dot{\varepsilon}^{p}_{ii}$ is the plastic part of the strain rate tensor and A is parameter concerning to initiation of the secondary-voids [6].

The critical void volume fraction f_c, determined on a round smooth specimen, was used to predict the onset of crack growth on the single-edge notched bend SE(B) and on the compact tension, C(T) specimens in this work.

3. Materials and experimental procedure

The base metal (BM) made of high-strength low-alloyed (HSLA) steel was used in a quenched and tempered condition. The fluxed-cored arc-welding (FCAW) process in shielding gas was used and two different fillers were used to have over-matching (OM) and under-matching (UM) weld metal. The chemical composition and mechanical properties of used materials are given in Table 1 and 2, respectively. The mismatching factor M is defined as;

$$M = \frac{R_{P0.2WM}}{R_{P0.2BM}} \tag{6}$$

where $R_{P0.2WM}$, and $R_{P0.2BM}$ are yield stresses of weld and base metal respectively.

Table 1. Chemical composition of base metal and fillers in weight [%]

Material	C	Si	Mn	P	S	Cr	Mo	Ni
Filler-OM	0.04	0.16	0.95	0.01	0.02	0.49	0.42	2.06
Base metal	0.123	0.33	0.56	0.003	0.002	0.57	0.34	0.13
Filler-UM	0.096	0.58	1.24	0.013	0.16	0.07	0.02	0.03

Table 2. Mechanical properties of base metal and weld metals (OM and UM) at room temperature.

Material	E [GPa]	$R_{p0.2}$ [MPa]	R_m [MPa]	M
Over-matching	183.8	648	744	1.19
Base metal	202.9	545	648	-
Under-matching	206.7	469	590	0.86

The damage parameters of materials such as; initial void volume fraction, f_0, for non-metallic inclusion and mean free path, λ, between non-metallic inclusions were estimated in [8]. The effect of secondary voids on ductile fracture was neglected based on, those secondary voids formed around Fe_3C particles have extremely low effect and present only during final stage of ductile fracture [8].

The critical void volume fraction values, f_c, (Table 3) is determined by combined experimental-numerical results from void volume fraction - round tensile (RT) diameter reduction curve. The value of critical void fraction, f_c, is determined corresponding to the experimental diameter reduction at final fracture [7].

The Gurson parameters of HSLA steel are given in Table 3 for over-matched, OM, and under-matched UM, weld metal

Table 3. Gurson parameters of HSLA steel.

Material	f_0	f_c	q_1	q_2
OM-WM	0.002	0.0173	1.5	1
UM-WM	0.002	0.0238	1.5	1

Mechanical tests were conducted at room temperature. The true stress-true strain diagrams are shown in Figure 1. Two welded joints of SE(B) and C(T) specimens were used (Figures 2 and 3). The geometry of SE(B) is given in [7]. The SE(B) specimen was fatigue precracked and the ratio of crack length to specimen width was $a_0/W = 0.32$ for both specimens SE(B) and C(T).

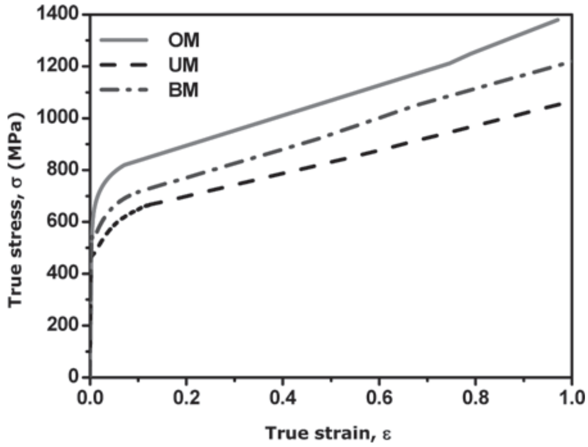

Figure 1. True stress-true strain curves of used materials.

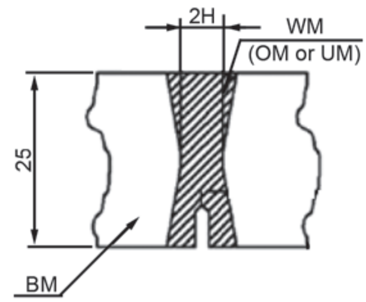

Figure 2. Welded joint of SE(B) specimen.

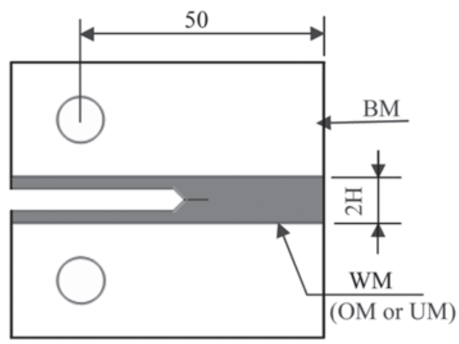

Figure 3. Geometry of welded C(T) specimen.

Welded joints are considered as bimaterials joints, since the crack is located in the weld metal, along the axis of symmetry of the weld. Two different widths of weld metal for both OM and UM welded joints were used: 2H = 6 and 12 mm as shown in Figures 2 and 3.

4. Numerical modelling of welded specimens

The FEM program (ABAQUS) was used with integrated yield criterion for determination of the value of stress and strain components and the value of f at non-linear behaviour. The specimens were analysed under plane-strain conditions, and 8-noded isoparametric reduced integration elements were used.

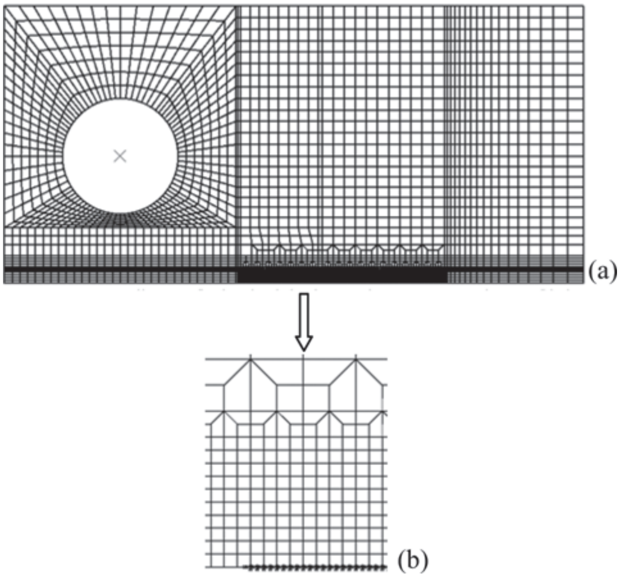

Figure 4. FE mesh of C(T) specimen (a), Crack - tip mesh (b).

The FE mesh size (0.15 x 0.15 mm) of SE(B) and C(T) specimens approximates to the estimated value of the mean free path λ between non-metallic inclusions were used, Figure 4 shows FE mesh of C(T) specimen with magnification of the mesh near the crack tip while FE mesh of SE(B) specimen is given in [7]. Due to symmetry of SE(B) and C(T) specimens, half of the specimens were modelled.

5. Results and discussion

5.1. Prediction of crack growth initiation

The values of critical void volume fraction, f_c, determined on the round tensile, RT, specimens were used for prediction of crack growth initiation on the SE(B) and C(T) specimens. The crack growth initiation on a precracked geometry is defined by the instant when the first element in front of the crack tip becomes damaged. It is shown in [8], that the condition for the onset of crack growth as determined by the J-integral at initiation, J_i, is most adequately defined by the micro-mechanical criterion:

$$f \geq f_c \tag{7}$$

The onset of the crack growth occurs when the condition given by Eq. (7) is satisfied. The crack growth initiation described here by crack tip opening displacement (CTOD$_i$) at crack growth initiation has been determined for OM and UM weld metals on C(T) specimen, that corresponding to critical void volume fraction, f_c (Figures 5 and 6). The experimental and numerical obtained values of CTOD$_i$ for OM and UM weld metal in case of 6 and 12 mm weld metal widths on SE(B) and C(T) specimens are given in Table 4.

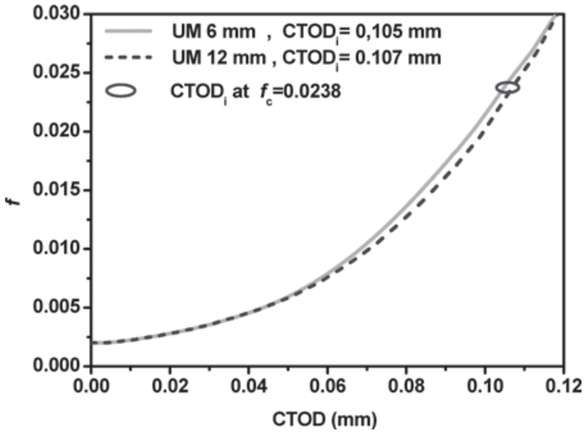

Figure 5. Void volume fraction, f, vs. crack tip opening displacement, CTOD, for C(T) specimens with two different widths of UM weld metal.

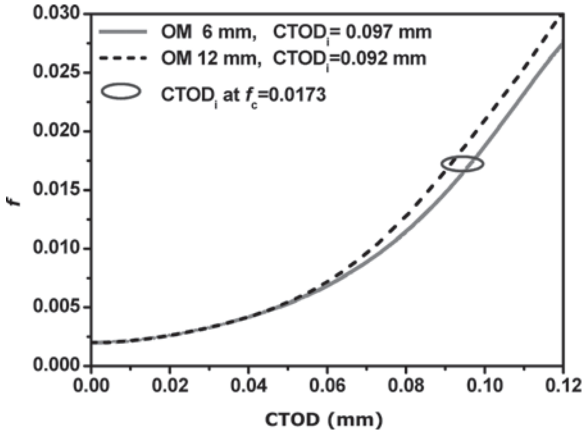

Figure 6. Void volume fraction, f, vs. crack tip opening displacement, CTOD, for C(T) specimens with two different widths of OM weld metal

Table 4. Experimental and numerical values of CTOD$_i$ for SE(B) and C(T) specimens in case of OM- over-matching, UM- under-matching

Specimen type		CTOD$_i$ (mm)			
		2H = 6 mm		2H = 12 mm	
		Exper.	Num.	Exper.	Num.
SE(B)	OM	0.092	0.110	0.084	0.106
	UM	0.12	0.124	0.124	0.129
C(T)	OM	-	0.097	-	0.092
	UM	-	0.105	-	0.107

It can be seen from Table 4, the values of CTOD$_i$ for C(T) specimen are more conservative than the values of SE(B) specimen. The results of SE(B) specimen are in good agreement with experimental one in case of UM, but in case of OM joints, there are some deviations which may be due to a small fraction of cleavage occurred in welded joint [7]. Moreover, the effect of strength mismatching and the width of weld metal can be predicted successfully by using GTN model. It is noticeable also; the higher resistance to ductile fracture initiation was obtained in OM welded joints with smaller width of weld metal, while the resistance to ductile fracture initiation of UM welded joints increases with the increase of width of weld metal, these obtained results are in agreement with the experimental one given in [9].

5.2. Evaluation of constraint level in welded specimens

In the present investigation, the constraint levels based on stress triaxiality are compared along ligament. Figures 7, 8 and 9 illustrate variation of stress triaxility due to variation of specimen geometry with loading condition, strength mismatching and width of weld metal, respectively. One can notice from Figure 7, the stress triaxiality level of C(T) specimen at crack tip is approximately similar to the stress triaxiality of SE(B) specimen, therefore the values of $CTOD_i$ for C(T) specimen close to the values of SE(B) specimen in cases of OM and UM (Table 4). It is noticeable also in Figures 7, 8 and 9, the most influence on stress triaxiality at crack growth initiation is dominant to specimen geometry with loading condition, strength mismatching and weld metal width respectively. Moreover, Figure 10 illustrates the higher opening stress, σ_{22} at initiation is for C(T) specimen with comparing to SE(B) specimen due to the effect of constraint.

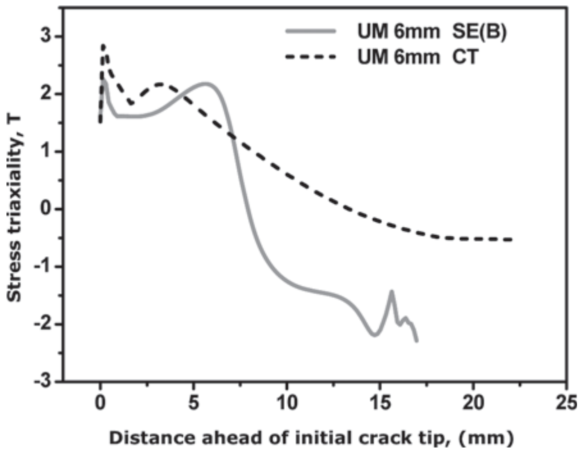

Figure 7. The variation of stress triaxiality along ligament due to variation of specimen geometry with loading condition in case of UM welded joints with 6mm weld metal width for SE(B) and C(T) specimens.

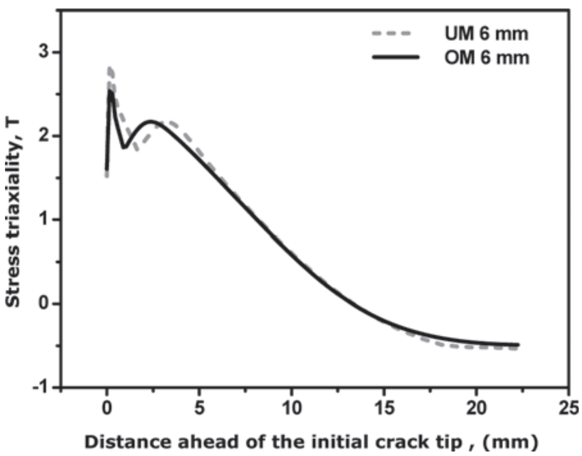

Figure 8. The variation of stress triaxiality along ligament due to the variation of strength mismatching in case of 6mm weld metal width for C(T) specimen

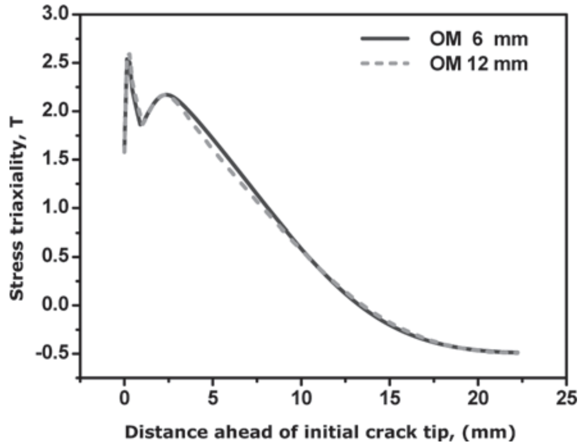

Figure 9. The variation of stress triaxiality along ligament due to variation of width of weld metal in case of OM for C(T) specimen.

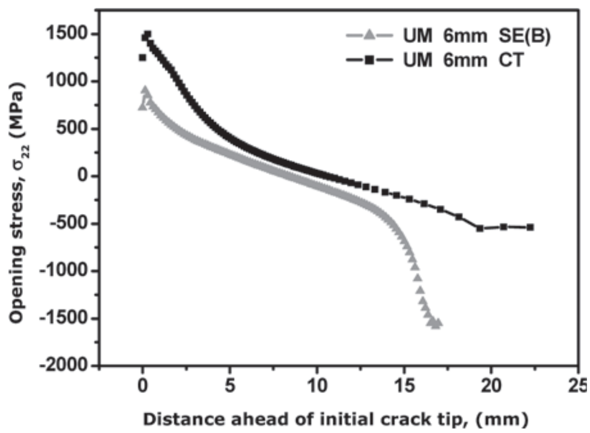

Figure 10. Opening stress along ligament for SE(B) and C(T) specimens in case of UM with 6mm weld metal width.

From the available literature [10], based on quantifying the level of constraint, if the triaxial conditions are found to be similar, then it is believed that crack growth initiation values $CTOD_i$ are transferable within certain circumstances. These conditions are evident for the geometries where the ligament length is large in the case of bending geometries and geometries that are predominately under tension. To compare the stress triaxiality of the specimen and components, one should take in account the remaining ligament which should be considered for the comparison, some investigations [10] indicated that the critical distance from the crack tip where cleavage fracture initiation occurs is within the range of J/σ_0 - $5J/\sigma_0$ (J is the J-integral and σ_0 is the yield stress), therefore the proper specimens for structural integrity assessment can be selected according to constraint level, if the constraint level of specimen matches the constraint level of component, the results of specimen seem to be transferred to that component within certain circumstances.

6. Conclusion

Ductile fracture initiation of welded specimens made of high-strength low alloyed steel has been investigated by using micromechanical GTN model. SE(B) and C(T) welded specimens were used to analyse ductile fracture behaviour by predicting the crack growth initiation and the effect of constraint level due to the variation of specimen geometry with loading condition, weld metal width and strength mismatching. The transferability of results from one component to another has been analysed on basis of stress triaxiality to find a way how ductile fracture parameters can be transferred from specimens to components. One can conclude, the GTN model can predict the ductile fracture initiation $CTOD_i$ of welded specimens and effect of constraint level based on critical void volume fraction, f_c. Ductile fracture initiation parameters such as $CTOD_i$ can be transferred from component to another within certain circumstances if their triaxial conditions are similar as can be noticed between SE(B) and C(T) welded specimens, therefore to transfer ductile fracture parameters from specimens to components, one should choose the proper specimen which has constraint level similar to component.

References

[1]. Gurson Al.: Continuum theory of ductile rupture by void nucleation and growth, part I. yield criteria and flow rules for porous ductile media, J Engng Mater Tech. 1977;99: pp. 2-15.

[2]. Tvergaard V., Needleman A.: Analysis of cup-cone fracture in a round tensile bar , Acta metal 1984; 32: pp. 57-169.

[3]. Thomason P. F.: Ductile fracture of metals, Pergamon press. Oxford. 1990.

[4]. Bauvineau L., Burlet H., Eripret C., Pineau A.: Modelling of ductile stable crack growth in a C-Mn steel with local approach , Paris, 1996. pp. 22-32.

[5]. Tvergaard V.: Influence of voids on shear bands instabilities under plane strain conditions, Int. J. Fract. 1981; 17: pp. 389-407.

[6]. Chu C., Needleman A.: Void nucleation effects in biaxiality stretched sheets, J. Engng Mater. Technol.. 1980; 102: pp. 249-256.

[7]. Rakin M., Gubeljak N., Dobrojevic M., Sedmak A.: Modelling of ductile fracture initiation in strength mismatched welded joint, Engng Fract. Mech. 2008; pp. 3499-3510.

[8]. Rakin M., Cvijovic Z., Grabulav V., Putic S., Sedmak A.: Prediction of ductile fracture initiation using micro-mechanical analysis , Engng Fract. Mech. 2004; 71: pp. 813-827.

[9]. Gubeljak N., Scheider I., Kocak M., Predan J.: Constraint effect on fracture behaviour or strength mismatched weld joint, In: 14 European Conference on Fracture, EMAS publishing, 2002. pp. 647-655.

[10]. Parankumar T.V., Chattopadhyay J., Dutta B.K., Kushwaha H.S.: Transferability of specimen J-R curve to straight pipes with through-wall circumferential flaws, Pressure vessel and piping, 2002; 79: pp. 127-134.